Molecular Therapy
Oncology
Original Article

Combining the constitutive TRAIL-secreting induced neural stem cell therapy with the novel anti-cancer drug TR-107 in glioblastoma

Morrent Thang,[1,2] Clara Mellows,[2] Lauren E. Kass,[2] Sabrina Daglish,[3] Emily M.J. Fennell,[3] Breanna E. Mann,[2] Alison R. Mercer-Smith,[2] Alain Valdivia,[2] Lee M. Graves,[3] and Shawn D. Hingtgen[1,2]

[1]Neuroscience Center, University of North Carolina—Chapel Hill School of Medicine, Chapel Hill, NC, USA; [2]Division of Pharmacoengineering and Molecular Pharmaceutics, University of North Carolina—Chapel Hill School of Pharmacy, Chapel Hill, NC, USA; [3]Department of Pharmacology, University of North Carolina—Chapel Hill School of Medicine, Chapel Hill, NC, USA

Tumor-homing neural stem cell (NSC) therapy is emerging as a promising treatment for aggressive cancers of the brain. Despite their success, developing tumor-homing NSC therapy therapies that maintain durable tumor suppression remains a challenge. Herein, we report a synergistic combination regimen where the novel small molecule TR-107 augments NSC-tumor necrosis factor-related apoptosis-inducing ligand (TRAIL) therapy (hiNeuroS-TRAIL) in models of the incurable brain cancer glioblastoma (GBM) *in vitro*. We report that the combination of hiNeuroS-TRAIL and TR-107 synergistically upregulated caspase markers and restored sensitivity to the intrinsic apoptotic pathway by significantly downregulating inhibitory pathways associated with chemoresistance and radioresistance in the TRAIL-resistant LN229 cell line. This combination also showed robust tumor suppression and enhanced survival of mice bearing human xenografts of both solid and invasive GBMs. These findings elucidate a novel combination regimen and suggest that the combination of these clinically relevant agents may represent a new therapeutic option with increased efficacy for patients with GBM.

INTRODUCTION

Glioblastoma (GBM) is a World Health Organization grade IV, deadly cancer of the central nervous system in adults.[1,2] GBM develops rapidly from mutated glial cells, carrying a poor median survival time of 12–15 months even with aggressive standard-of-care treatments consisting safe maximal surgical resection with adjuvant chemotherapy and radiation therapy.[3] Due to the aggressive characteristics of GBM, tumor recurrence is nearly universal in patients and there are no established standard-of-care treatments for GBM recurrence.[4,5] Thus, more effective therapies are urgently needed to overcome the notorious heterogeneity-induced complications in GBM treatment to increase the survival outcomes for patients.

A promising therapy for the treatment of a plethora of cancers is tumor necrosis factor-related apoptosis-inducing ligand (TRAIL).[6,7] TRAIL binds to death receptors 4 and 5 (DR4 or TRAIL-R1 and DR5 or TRAIL-R2) on the surface of tumor cells and activates extrinsically mediated apoptotic pathways without harming normal cells significantly.[8] Upon binding, the TRAIL/DR complex undergoes homotrimerization, resulting in intracellular domain forming a death-inducing signaling complex, consisting of an adaptor molecule, Fas-associated death domain and pro-caspase 8.[9] The activated caspase 8 then cleaves effector caspases 3 and 7 and ultimately induces apoptosis in cancer cells. Previous studies suggest that this selectivity against cancer cells may be due to the inherent overexpression of DRs in cancer cells and lower expression of DRs in normal cells.[8] However, other findings contradicted that the level of DR expression may not dictate the specificity in TRAIL-mediated cell death.[10,11] Nonetheless, the clinical application of TRAIL is promising as the pro-apoptotic protein activates a different apoptotic pathway than many existing chemotherapies—most chemotherapeutics rely on the activity of the intrinsic-mediated apoptotic protein, tumor suppressor p53.[9] However, p53 can become inactivated or dysregulated frequently in GBM,[12] leading to resistance in apoptosis and decreasing the efficacy of subsequent rounds of chemotherapy.[13] Thus, TRAIL could be incorporated instead of or concurrently with other chemotherapies to augment overall treatment durability, especially in p53-mutated GBM tumors.[14]

Unfortunately, TRAIL and TRAIL-based therapies have been unsuccessful in clinical trials against several cancers, likely due to its short half-life (<1 h in serum), leading to insufficient TRAIL accumulation at the tumor region and to the pre-existing or acquisition of TRAIL resistance by cancer cells.[15,16] Therefore, we aimed to address these limitations by first increasing TRAIL bioavailability at the tumor site using our engineered tumor-homing stem cells that continuously secrete TRAIL proteins, and second by combining it with a secondary therapy—a novel anti-cancer compound TR-107.

Received 24 August 2023; accepted 13 June 2024;
https://doi.org/10.1016/j.omton.2024.200834.

Correspondence: Shawn D. Hingtgen, Neuroscience Center, University of North Carolina—Chapel Hill School of Medicine, Chapel Hill, NC, USA.
E-mail: hingtgen@email.unc.edu

Human induced neural stem cells (hiNSCs) emerged as attractive biotherapeutic carriers due to their innate ability to migrate to tumors via chemotactic signaling, potentially involving CXC chemokine receptor type 4 on hiNSCs and vascular endothelial growth factor, stromal cell derived factor 1, and urokinase-type plasminogen activator secreted from the tumor microenvironment.[17,18] Our lab has recently developed the next generation of hiNSCs, called spheroidal induced NSCs (hiNeuroS), which have demonstrated robust tumor tropism and persistence in the brain, providing an ideal vehicle to deliver antitumor therapies.[19] Furthermore, personalized therapeutic cells have decreased the risk of patients' immune rejection since they can be generated autologously from patients' own skin fibroblasts—displaying immense clinical potential—as opposed to allogenic stem cells, which can elicit unwanted immune responses in patients and increase clearance.[20,21] We have shown that mice treated with hiNeuroS cells engineered to secrete TRAIL (hiNeuroS-TRAIL) exhibited significantly reduced tumor growth in several murine models of brain metastases.[18,19] However, this study is the first to investigate the effects of hiNeuroS-TRAIL in GBM.

Although sufficient accumulation of TRAIL protein at the tumor site is ideal, GBM cells can possess innate TRAIL resistance, or they can acquire TRAIL resistance and evade apoptosis.[22] Therefore, one method to improve hiNeuroS-TRAIL therapy is to decrease the risk of resistance in GBM cells by targeting other aspects of the apoptosis simultaneously by adding a secondary therapy to further sensitize cancer cells to TRAIL. TR-107 is a novel experimental compound that has shown potential for significant tumor reduction and survival extension in a murine model of triple negative breast cancer (TNBC).[23] TR-107 is an analog of ONC201, the first imipridone drug to have advanced to phase 3 clinical trials for adult and pediatric patients with deadly H3 K27M-mutated midline gliomas.[24] Although very similar in chemical structure, TR-107 is approximately 200× more potent than ONC201 in cancer growth inhibition assays.[23]

ONC201 has been proposed to exert its anti-cancer effects by both acting as a dopamine receptor 2 (DRD2) antagonist and a caseinolytic mitochondrial matrix peptidase proteolytic (ClpP) activator (ClpP agonist) in cancer cells.[25] DRD2 is a G protein-coupled neuroreceptor that is essential in regulating Ras signaling, which is vital for cellular growth.[26–28] By antagonizing DRD2, ONC201 is believed to inhibit tumor growth by impeding the Ras signaling pathway in various cancer cells.[26,27] ClpP is a mitochondrial protease that canonically degrades misfolded proteins in the mitochondria.[28] When activated by ClpP agonists (e.g., ONC201, TR-107, and other TR compounds), ClpP undergoes conformational change,[29,30] resulting in excess degradation of mitochondrial proteins that are essential for tumor growth.[28] While both ONC201 and the TR compounds directly bind and activate ClpP, there is no evidence for DRD2 antagonism by the TR compounds.[28,29,31,32]

ONC201 also upregulates TRAIL and DR5 proteins in several cancer cell lines,[27] and synergizes with TRAIL-based therapies and other small molecule inhibitors in tumor killing.[33–36] Although not previously explored in GBM, TR-107 has been shown to be significantly more potent than ONC201 in inhibiting TNBC cell growth via a ClpP-dependent mechanism. In these cells, activation of ClpP disrupts oxidative phosphorylation and decreases cancer cell proliferation.[23] Thus, these findings suggest the potential for TR-107 as a candidate to combine with hiNeuroS-TRAIL, to exhibit synergistic tumoricidal effects and overcome TRAIL resistance in GBM by targeting metabolic adaptations that favor drug resistance.[37]

Herein, we provide a study of hiNeuroS-TRAIL and TR-107 combination approaches to assess the therapeutic effects with *in vitro* and *in vivo* platforms of established human GBM cells and patient-derived primary GBM cells with different TRAIL sensitivities.[38] We first investigated the *in vitro*, dose-dependent effects for both therapies in GBM cell lines and combined the optimal doses of each therapy to further conduct synergy studies. Next, to identify the molecular markers involved in combination-induced tumor growth suppression *in vitro*, we profiled apoptotic signaling pathways modulated by single agents or in combination using caspase and apoptotic arrays in TRAIL-resistant LN229 cells. Finally, to assess the efficacies of both therapies for potential clinical application, we developed a combination therapy in both solid and invasive orthotopic murine models of GBM and monitored for tumor growth and survival outcomes.[39]

RESULTS

Combining TR-107 and hiNeuroS-TRAIL synergistically suppresses growth of multiple GBM cell lines

Previous studies reported synergy of growth inhibition when combining TRAIL-inducing ONC201 with a DR5 agonist and other small molecules.[33–36] Based on these studies, we hypothesized that the combination of hiNeuroS-TRAIL and the ClpP agonist TR-107 would synergize in inhibiting GBM tumor growth. To assess this treatment for potential synergy, we first conducted dose-response experiments to establish the efficacy of the single agent TR-107 and hiNeuroS-TRAIL using established and primary human GBM cell lines with different sensitivities to TRAIL. Using cell viability assays, we found that the median inhibition concentration (IC_{50}) of TR-107 ranged from 50 to 100 nM in two of the GBM cell lines (Figures 1A and 1B). The IC_{50} values obtained with hiNeuroS-TRAIL treatment of LN229 and MS21 was approximately 5.0×10^3–1.0×10^4 cells (Figures 1D and 1E). Based on these values and the non-toxicity of TR-107 toward hiNeuroS-TRAIL cells (Figure S1A), we selected 100 nM TR-107 to test in combination with hiNeuroS-TRAIL cells. As TRAIL-secreting hiNeuroS cells are persistent and proliferative, we chose 5.0×10^3 hiNeuroS-TRAIL cells to combine with TR-107 for studies in LN229 and MS21 cells. GBM8 cells seemed to be extremely sensitive to both therapies, requiring lower amounts of TR-107 (15 nM) as well as amounts of hiNeuroS-TRAIL (5.0×10^2) than the other two cell lines (Figures 1C and 1F). Based on these analyses, we observed synergistic cell growth inhibition in all three GBM cell lines. Compared with the control or single agent treatment groups ($p < 0.0001$) (Figures 1G–1I), the coefficient of drug interaction (CDI) values were 0.67, 0.60, and 0.15 in LN229, MS21, and GBM8 respectively, indicating that synergy of growth was achieved in these GBM cell lines *in vitro*.

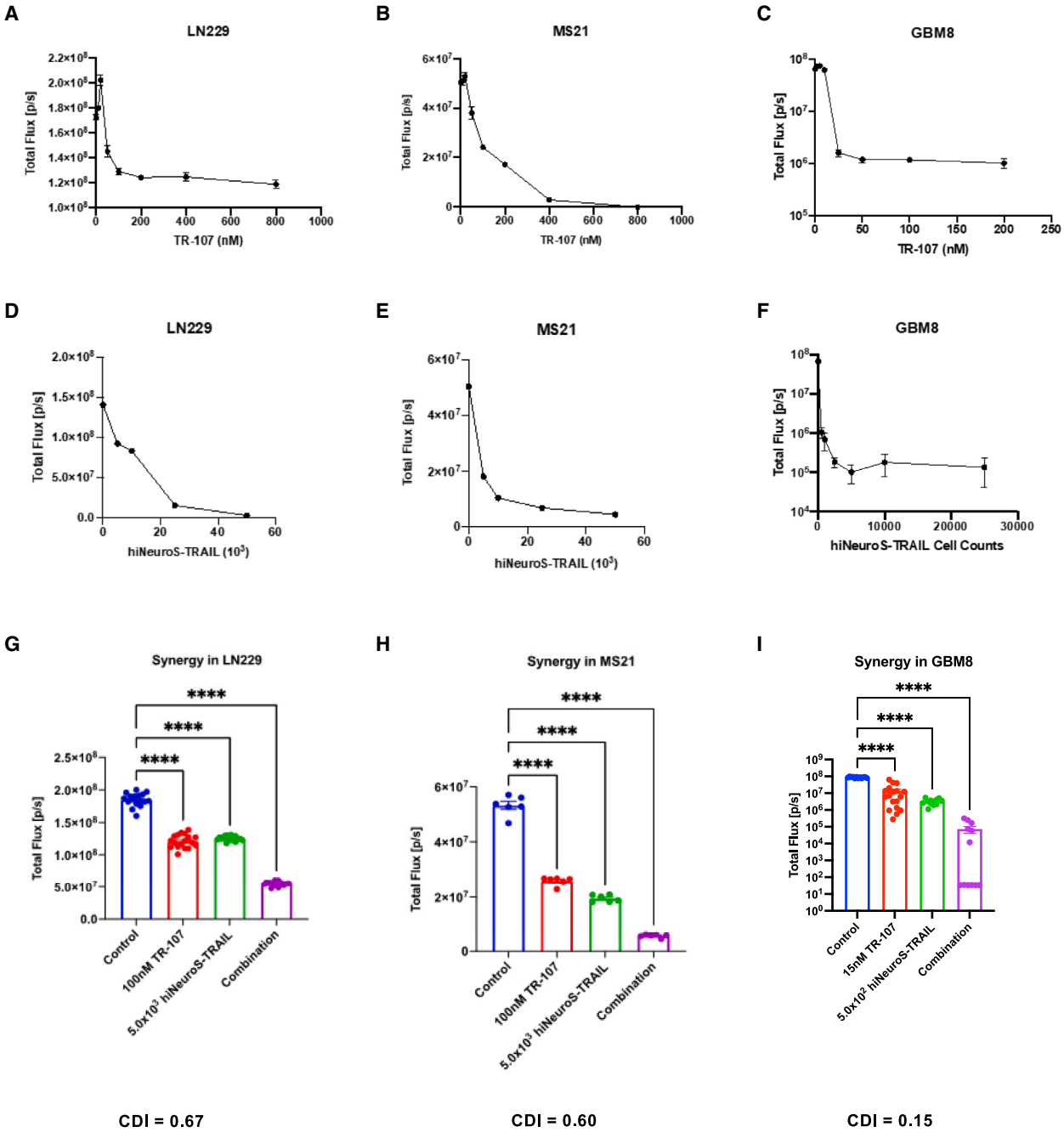

Figure 1. Combining TR-107 and hiNeuroS-TRAIL demonstrates synergistic tumor growth suppression in various GBM cell lines

(A–C) TR-107 dose-response curve in (A) LN229 (B) MS21 and (C) GBM8 (log scale) (n = 6). (D–F) hiNeuroS-TRAIL dose-response curve in (D) LN229 (E) MS21 and (F) GBM8 (log scale) (n = 6). (G–I) Combining IC_{50} doses of both drugs demonstrate synergistic inhibition of tumor growth in (G) LN229 (n = 18) (H) MS21 (n = 6) and (I) GBM8 (log scale) (n = 12–18 for all cell lines). The data are represented as mean ± SEM (****$p < 0.0001$).

TR-107 treatment activates caspase-mediated apoptotic signaling pathways in the TRAIL-sensitive cell line, GBM8

As we observed synergistic growth inhibition in GBM cell lines, we next investigated the molecular mechanism underlying this effect. Since TRAIL-mediated cell death has been shown to occur through activation of the extrinsic apoptotic pathway, we examined the impact of TR-107 on both the intrinsic and extrinsic apoptotic signaling pathways.[40,41] We first performed a 24-h dose-response assay of

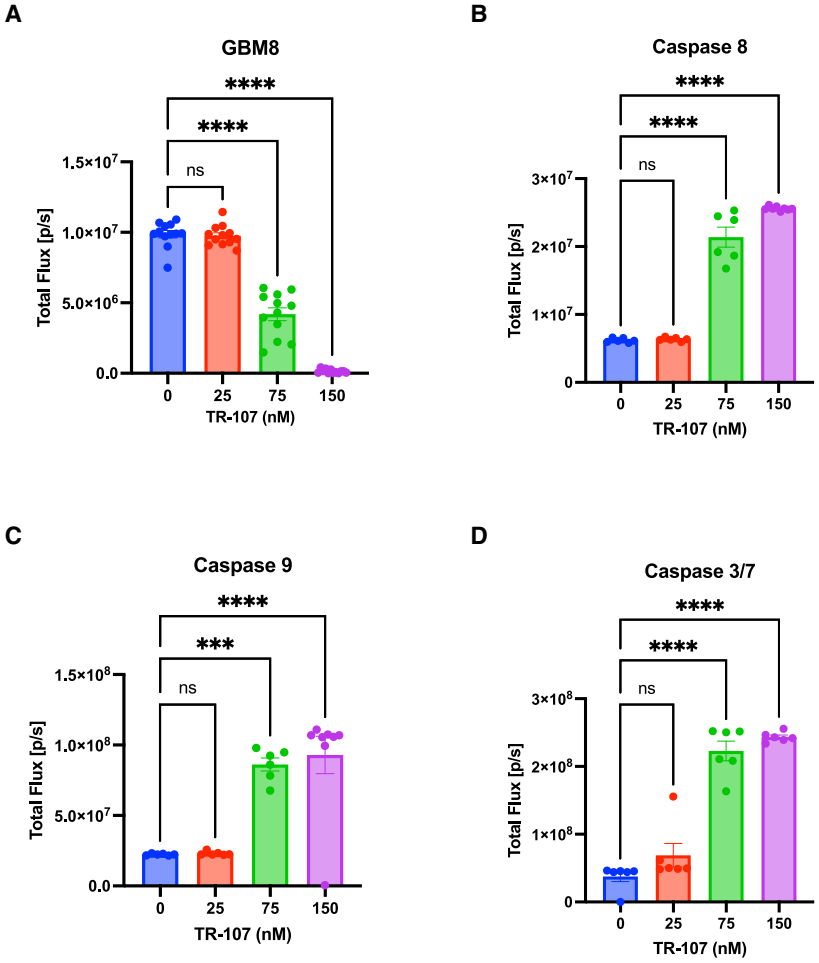

Figure 2. TR-107 treatment activates caspase-mediated apoptotic signaling pathway in TRAIL-sensitive cell line, GBM8

(A) GBM8 tumor growth curve in response to TR-107 treatments (n = 12). (B) Extrinsic-mediated caspase 8 regulation (n = 6–8). (C) Intrinsic-mediated caspase 9 regulation (n = 6–8). (D) Extrinsic and intrinsic-mediated caspase 3/7 regulation (n = 5–6). The data are represented as mean ± SEM (***$p < 0.001$, ****$p < 0.0001$, ns = not significant).

TR-107 treatment in TRAIL-sensitive cell line, GBM8, and observed that GBM8 growths were unaffected at 25 nM but were inhibited at 75 nM and 150 nM of TR-107 concentrations (Figure 2A). We also observed that all caspases associated 3/7, 8, and 9 were upregulated significantly at these cytotoxic doses (Figures 2B–2D), indicating that TR-107 activates the caspase-mediated apoptotic signaling pathways in TRAIL-sensitive GBM8 cells.

Combining hiNeuroS-TRAIL and TR-107 therapies significantly elevate increase activation in LN229

Next, we performed time-dependent (24- and 48-h) hiNeuroS-TRAIL/TR-107 combination experiments using the TRAIL-resistant GBM cell line, LN229, as a positive control (Figure 3A).[38] We then performed caspase activity assays for caspases 3/7, 8, and 9 to examine both intrinsic and extrinsic apoptotic pathways at the 24- and 48-h timepoints. Consistent with the literature, hiNeuroS-TRAIL treatment alone upregulated multiple markers of caspase activation (Figures 3B–3D). By contrast, TR-107 alone did not induce an increase in caspase markers in 24 and 48 h after treatment (Figures 3B–3D). Although TR-107 alone did not affect caspase activation, combination with TR-107 enhanced hiNeuroS-TRAIL stimulated caspase upregulation in LN229 cells. This combination treatment induced a significant increase in caspase activity compared with the control and single-agent treatment groups (Figures 3B–3D), the results of which were more robust after 48 h. Comparing the caspase assay results (caspases 3/7, 8, and 9) suggested that both the intrinsic and extrinsic pathways were affected by these treatments.

Combination treatment alters protein expression in a pro-apoptotic pattern in LN229

To further investigate the mechanism underlying the combined effects of TR-107 and hiNeuroS-TRAIL therapies in LN229 cell line, we used a human apoptotic array to identify potential molecular targets in the apoptotic pathways that may be modulated by these therapies individually or together (Figure 4A). The results of these studies validated our caspase data, which suggested that TR-107 does not directly impact the activity of caspase 3. By contrast, the hiNeuroS-TRAIL and the combination treatments both significantly upregulated caspase 3 activity compared with the control or TR-107 treatment groups (Figure 4B). In the array panel, the phosphorylation of p53 at different residues (S15 and S46) exhibited the greatest increase after combination treatment (Figures 4C and 4D). Furthermore, we discovered that combination treatment significantly downregulated two proteins from the inhibitors of the apoptotic proteins (IAPs) family, survivin and X-linked IAP (XIAP) (Figures 4E and 4F). Survivin and XIAP are well-characterized caspase inhibitory proteins that prevent cells from undergoing apoptosis.[42] As p53 is vital in initiating intrinsic signal-mediated apoptosis and IAPs are associated with evasion of apoptosis by radioresistance, chemoresistance, and TRAIL resistance in several cancers including GBM, these data suggest that the combination-induced synergy is due to enhanced regulation of both p53-mediated and TRAIL-mediated apoptosis in TRAIL-resistant LN229 cells.

Single-agent dose optimizations in solid GBM model in mice

Next, we wanted to determine whether the synergy observed *in vitro* could be observed in the *in vivo* models. To develop a

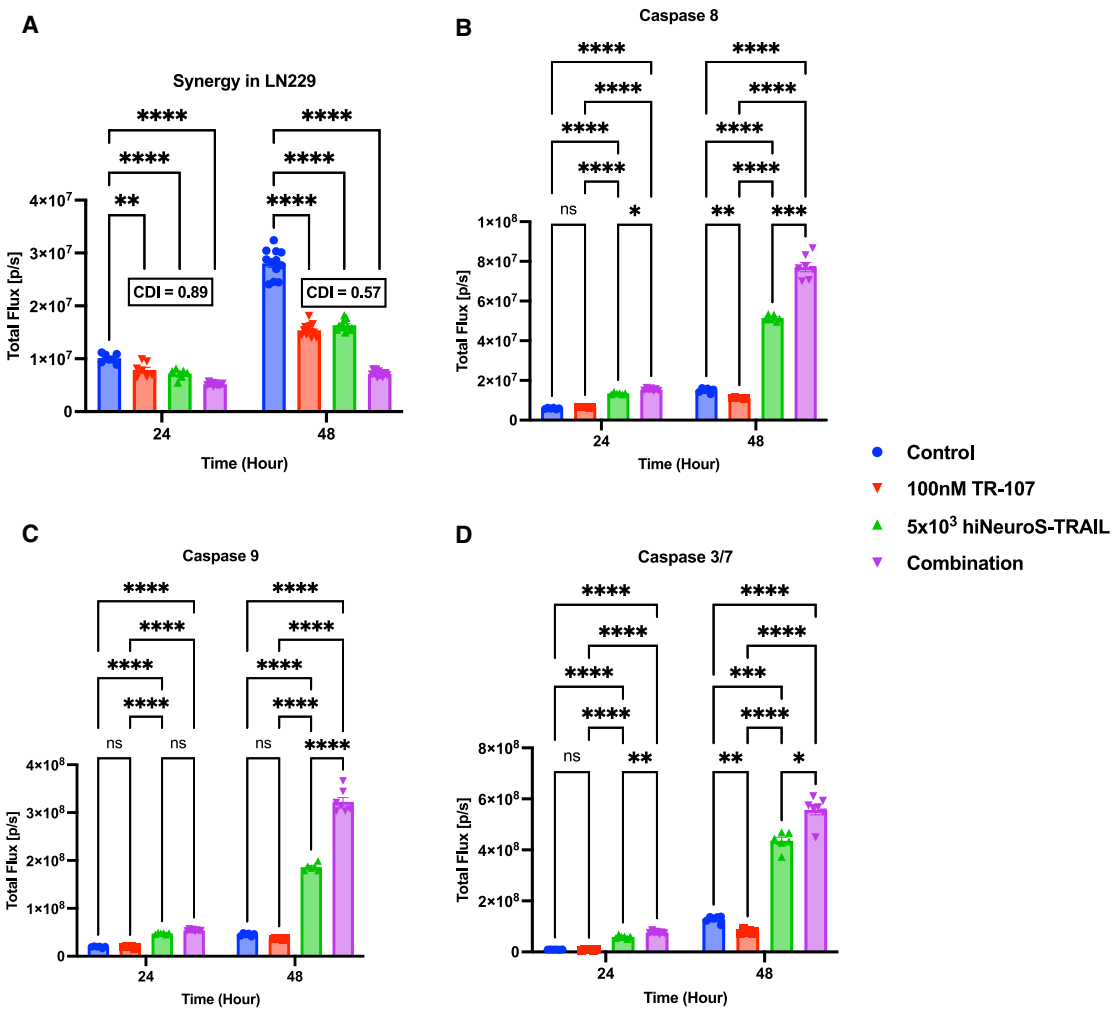

Figure 3. Combining TR-107 with hiNeuroS-TRAIL significantly upregulated caspase markers in TRAIL-resistant LN229 *in vitro*

(A) The 24- and 48-h synergistic tumor killings with CDI values of 0.89 and 0.57, respectively in LN229 cell line (n = 7–12). (B) Extrinsic-mediated caspase 8 regulation from 24 to 48 h in response to single agents and combination treatments (n = 6–7). (C) Caspase 9 regulation from 24 to 48 h in response to single agents and combination treatments (n = 6–7). (D) Extrinsic and intrinsic-mediated caspase 3/7 regulation from 24 to 48 h in response to single agents and combination treatments (n = 6–7). The data are represented as mean ± SEM (*$p < 0.05$, **$p < 0.01$, ***$p < 0.001$, ****$p < 0.0001$, ns = not significant).

combination therapy regimen, we first conducted pilot studies on individual therapies in the TRAIL-resistant LN229 model.[38] We found that, compared with the PBS control group (Figure 5A), six intermittent intraperitoneal (IP) injections of 5 mg/kg TR-107 significantly decreased the tumor burdens without obvious signs of toxicity (Figure 5B). In addition, we found that IP injections of 10 mg/kg induced signs of toxicity as two of the four mice reached the humane endpoints only a few days after the treatments were administered (Figure 5C). Although both TR-107 treatment groups demonstrated significant tumor growth decreases in LN229 tumor-bearing mice (Figure 5D), their survival outcomes were not improved (Figure 5E), suggesting a need for a continuous dosing regimen. For hiNeuroS-TRAIL pilot study, we administered PBS for control treatment (Figure 5F) and 1.0×10^5 cell counts for hiNeuroS-TRAIL therapy (Figure 5G) intratumorally (IT). Our cell-based TRAIL therapy showed a brief and significant tumor decrease on day 18 after administration (Figure 5H), followed by an improvement in survival rate compared with control mice (Figure 5I). However, due to a small sample size (n = 3), we remained consistent with a single IT injection of 1.0×10^5 hiNeuroS-TRAIL to combine with 5 mg/kg intermittent IP injections of TR-107 to evaluate the therapeutic efficacy of the combination therapy.

Assessing TR-107 and hiNeuroS-TRAIL combination therapy against solid GBM in mice

To assess the efficacy of the combination therapy in a murine model of solid GBM, we performed stereotactic implantations of 2.0×10^5

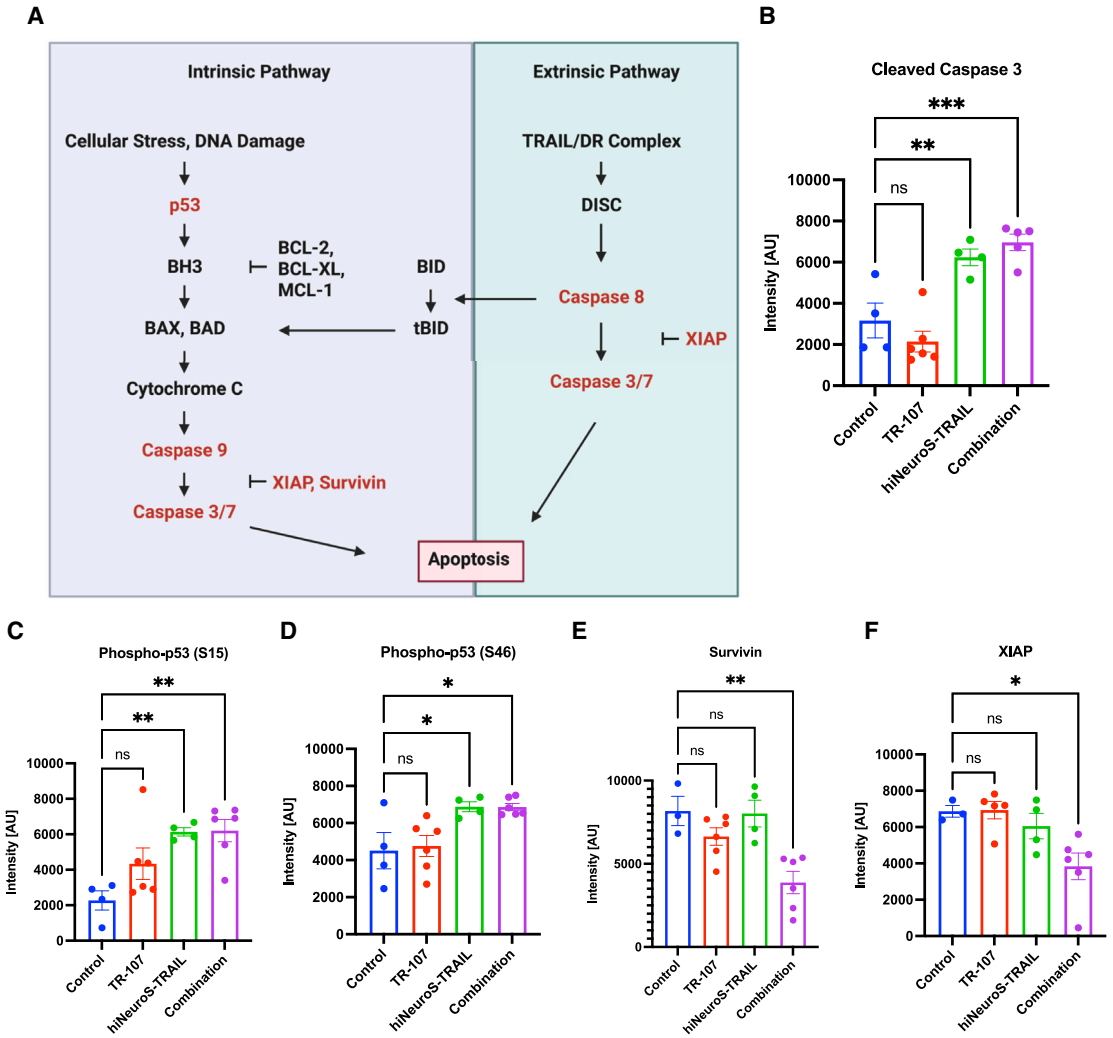

Figure 4. Combination treatment alters protein expression in the apoptotic pathways favoring the pro-apoptotic pattern in TRAIL-resistant LN229 cell line

(A) A schematic for intrinsic and extrinsic mediated apoptotic pathways. Molecular markers highlighted in red are differentially regulated in the experiment in response to treatments. (B–F) Proteomic differential expressions for (B) cleaved caspase 3 (C) p53 phosphorylation at S15 site (D) p53 phosphorylation at S46 site (E) survivin and (F) XIAP (n = 4–6). The data are represented as mean ± SEM (*$p < 0.05$, **$p < 0.01$, ***$p < 0.001$, ns = not significant).

LN299 cells in athymic female mice aged 6–8 weeks and randomized based on their tumor burdens to ensure that there were no significant differences in the measurements across all groups. The control mice received single IT injections of saline (PBS) on day 0, and six IP injections (days 0, 2, 4, 14, 16, and 18) of vehicle (5% Solutol and 5% DMSO in PBS). The TR-107 treatment group of mice received six IP injections (days 0, 2, 4, 14, 16, and 18) of 5 mg/kg TR-107 and the hiNeuroS-TRAIL treatment group of mice received single IT injections of 1.0×10^5 hiNeuroS-TRAIL on day 0. Finally, the combination treatment group of mice received single IT injections of 1.0×10^5 hiNeuroS-TRAIL on day 0 and six IP injections (days 0, 2, 4, 14, 16, and 18) of 5 mg/kg TR-107. Longitudinal bioluminescence imaging to track tumor burdens (Figures 6A–6D for tumor growth curves of each treatment group) demonstrated that the combination therapy markedly inhibited GBM progression, decreasing the tumor burden by 4-fold compared with control-treated animals or TR-107 alone at 4 weeks after treatment (mean fold change for controls, 23.1-fold; for combination therapy, 6.4-fold). This resulted in CDI values of 0.86 (day 22) and 0.75 (on day 27) after treatments, indicating synergistic therapeutic efficacies (Figure 6E). The enhanced tumor suppression led to a significant improvement in the overall median survival outcome, with survival in the combination group extended to 61 days compared with 48 days for the control, TR-107, and hiNeuroS-TRAIL groups (Figure 6F). Together, these data suggest that combining TR-107 and hiNeuroS-TRAIL augmented treatment durability by significantly decreasing tumor growth in LN229 GBM tumor-bearing mice and improving their overall survival outcome.

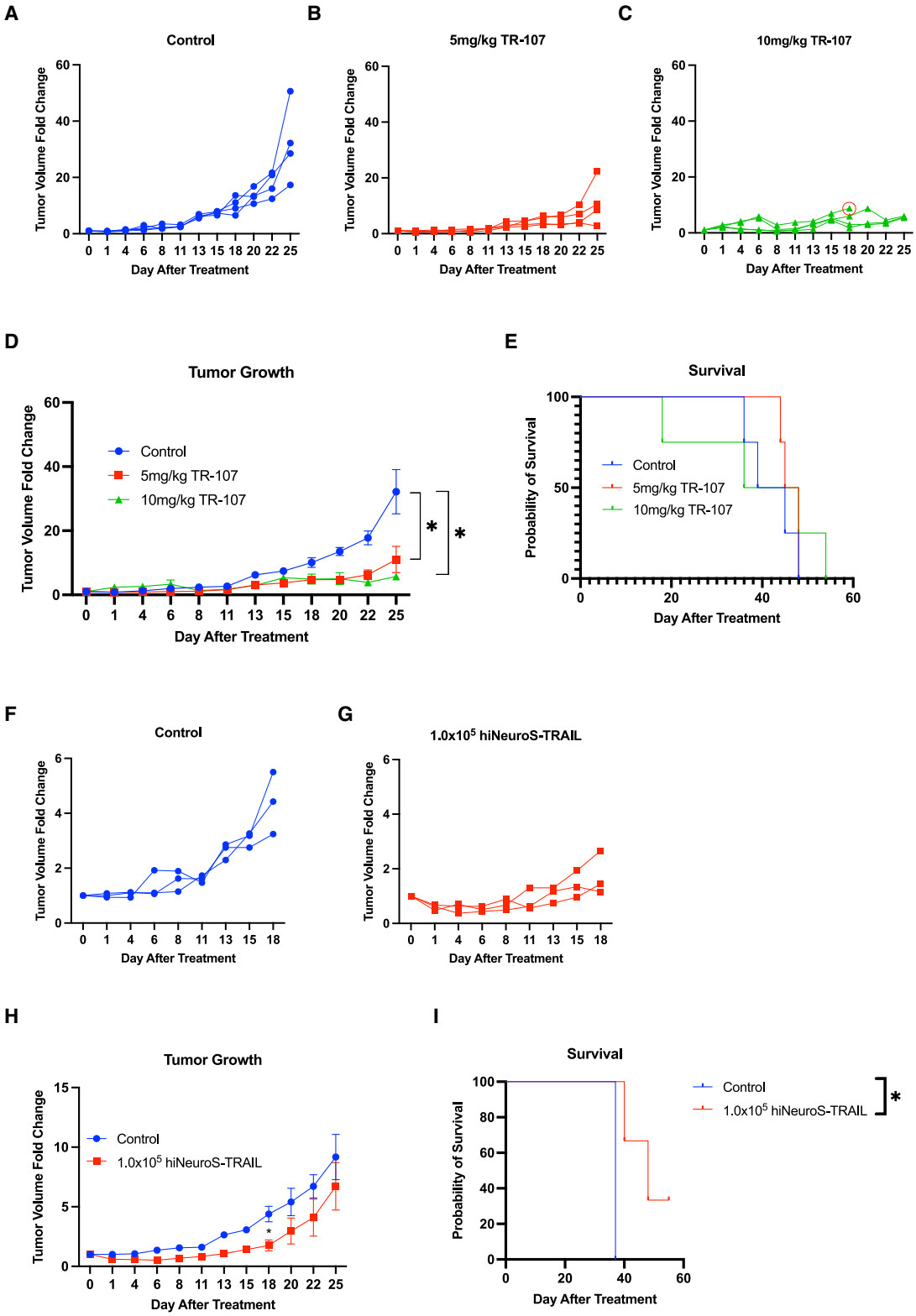

(legend on next page)

Assessing a TR-107 and hiNeuroS-TRAIL combination regime against established GBM in mice

Next, we explored the efficacy of the combination therapy in an *in vivo* murine model of invasive GBM.[39] Stereotactic implantations of 1.0×10^5 GBM8 neurosphere cancer cells was performed in athymic female mice aged 6–8 weeks and the mice were randomized based on their tumor burdens without significant differences across all treatment groups. The control mice received single IT injections of 1XPBS on day 0, and six IP injections of vehicle (5% Solutol and 5% DMSO in 1XPBS) on days 0, 2, 4, 14, 16, and 18 (until the last mouse reached a humane endpoint). TR-107 group of mice received IP injections of 5 mg/kg TR-107 on days 0, 2, 4, 14, 16, 18, 28, 30, 32, and 42 (until the last mouse reached a humane endpoint). hiNeuroS-TRAIL group of mice received single IT injections of 5.0×10^4 hiNeuroS-TRAIL on day 0. Finally, the combination group of mice received single IT injections of 5.0×10^4 hiNeuroS-TRAIL on day 0 and intermittent IP injections of 5 mg/kg TR-107 on days 0, 2, 4, 14, 16, 18, 28, 30, 32, 42, 44, 46, 56, 58, and 60. Due to the invasive and aggressive nature of GBM8 tumors in mice, three control mice reached humane endpoints on days 12, 14, and 15 after treatment. Longitudinal bioluminescence imaging and the analysis of the tumor burdens (Figures 7A–7D for tumor growth curves of each treatment group) demonstrated that there was no significant change in the tumor growth rate across all treatments (Figure 7E). However, we observed a significant improvement in the overall median survival outcome of the combination group (73.5 days) compared with the control group (15.5 days), TR-107 group (27 days), and hiNeuroS-TRAIL group (67 days) (Figure 7F). While there was no significant change in the tumor growth rate across all treatments with early humane endpoints in control and TR-107 groups, these results suggest that combining TR-107 and hiNeuroS-TRAIL significantly improved survival outcomes compared with control and single-agent therapy treated groups in an invasive murine model of GBM. Additionally, although the hiNeuroS-TRAIL alone group showed extended survival outcome of GBM8 tumor-bearing mice, combining with a secondary therapy (TR-107) while decreasing the therapeutic cell counts may prevent these invasive GBM cells from adapting to TRAIL and establishing resistance.

DISCUSSION

GBM is a deadly disease with no curable therapies to date.[1,4,5] Due to the heterogeneity of this devastating disease, combating GBM with a singular agent may not be the most effective treatment option for all patients.[43] Thus, it is critical to explore combination therapies that could result in synergistic or additive therapeutic responses against multiple cell lines in both clinically relevant *in vitro* cell lines and *in vivo* models.[44] Although TRAIL and TRAIL-based therapies possess paramount potential as anti-cancer therapy against GBM, further optimization is necessary to overcome the limitations that are associated with unsatisfactory results in clinical trials.

Herein, we examined the challenges associated with TRAIL-based therapies by harnessing our engineered induced NSCs for constitutive TRAIL secretion and further combining it with a recently characterized small molecule TR-107 in GBM. First, we demonstrated that, together, these therapies can synergistically inhibit tumor growth in both established and primary GBM cell lines at low cell counts and doses of hiNeuroS-TRAIL and TR-107, respectively. Second, we tested this combination approach in two well-established *in vivo* GBM models. The results of our studies strongly support the benefits of combining hiNeuroS-TRAIL cells with TR-107 both *in vitro* and *in vivo* models of GBM.

Although the mechanism of TRAIL protein as a therapeutic has been characterized extensively,[16,45,46] the underlying mechanisms of TR-107 in cancer cells are not fully understood. Recently, TR-107 was shown to target mitochondrial proteins required for tumor growth by activating the mitochondrial protease ClpP. Activation of ClpP results in the downregulation of multiple mitochondrial matrix proteins associated with oxidative phosphorylation, the tricarboxylic acid cycle function, and mitochondrial transcription as shown in TNBC cell lines.[23] However, aside from the ClpP dependence and regulation of mitochondrial proteins in TNBC cells, its effects on the apoptotic pathways have not been elucidated.

To better understand the TR-107-mediated apoptotic regulation in GBM *in vitro*, we assessed the levels of caspase markers in both TRAIL-sensitive and -resistant cell lines, GBM8 and LN229, respectively. First, we found that the TR-107 doses that are cytotoxic toward GBM8 cells upregulate caspase markers significantly, indicating that TR-107 induces cellular apoptosis in GBM8 cells. However, in LN229 cells, TR-107 alone intriguingly did not induce caspase activation at an IC_{50} dose, whereas hiNeuroS-TRAIL significantly upregulated the caspase proteins compared with the control. When combined, TR-107 interestingly bolstered the effect of hiNeuroS-TRAIL therapy as the combination treatment significantly increased the caspase proteins compared with all treatments. To further explore the mechanisms of enhanced apoptosis mediated by our co-treatment in TRAIL resistance, we characterized the apoptotic markers after single or combination treatment-induced effects in LN229 cells. Using an apoptotic array, we found that hiNeuroS-TRAIL treatment increased the phosphorylation of p53 at the S15 and S43 residues, suggesting activation of the intrinsic apoptotic pathway. The role of p53 is vital in activating intrinsic-mediated apoptosis—especially in radiation therapy and several chemotherapies as the phosphorylation of p53 subsequently results in interaction with the BCL-2 family that further induces

Figure 5. Single agent dose optimizations in solid LN229 GBM model in mice

(A–C) Individual mouse tumor growth curves across all control and TR-107 treatment groups. (D and E) (D) Fold change in tumor growth curve and (E) survival outcome across all TR-107 treatment groups (n = 4). (F and G) Individual mouse tumor growth curves across all control and TR-107 treatment groups. (H and I) (H) Fold change in tumor growth curve and (I) survival outcome between control and hiNeuroS-TRAIL treatment groups (n = 3). The data are represented as mean ± SEM (*$p < 0.05$).

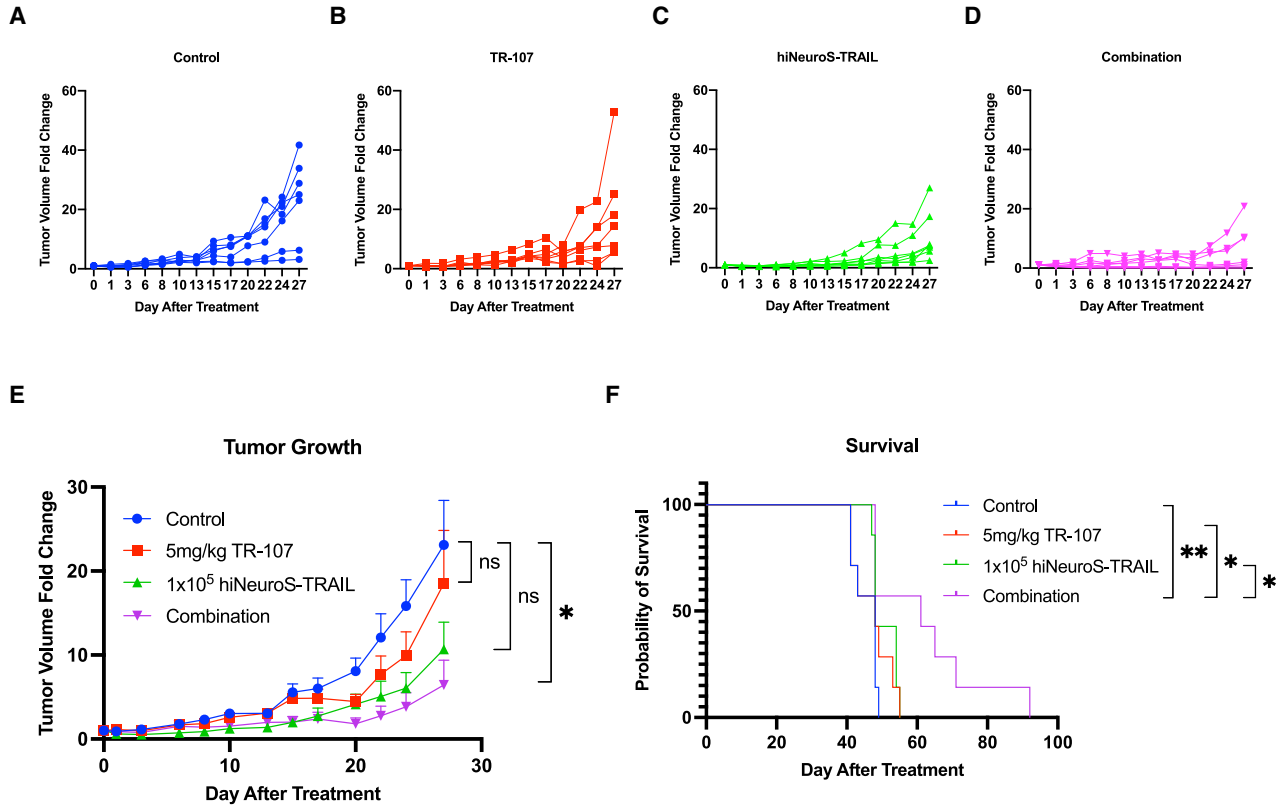

Figure 6. Combining TR-107 and hiNeuroS-TRAIL significantly reduced tumor burden and improved survival outcome in a solid murine model of GBM

(A–D) Individual mouse tumor growth data across all treatment groups from LN229 *in vivo* efficacy experiment. (E) Fold change in tumor growth curves across all treatment groups indicating that the combination therapy significantly reduced tumor burdens compared with the control group. (F) Kaplan-Meier survival curve of mice treated with control, TR-107, hiNeuroS-TRAIL, or combination at indicated doses (n = 7). The data are represented as mean ± SEM (*$p < 0.05$, **$p < 0.01$, ns = not significant).

apoptosis.[47] Hence, an increase in p53 phosphorylation indicates that these therapies in combination can promote both DR-mediated and mitochondrial-mediated apoptotic activities in the LN229 cell line.

Due to the limited literature on the role of TRAIL's effects on p53 phosphorylation (S15 and S46), we speculated that the outcome was due to the unexplored secretome of our hiNeuroS cells. Although hiNeuroS cells are engineered to solely secrete TRAIL proteins continuously, it is reasonable that these cells may inherently secrete additional factors that aid in the regulation of molecular markers in pro-apoptotic-favoring patterns. It has recently been reported that the adipose mesenchymal stem cell-derived secretome had an anti-tumor effect by modulating intrinsic apoptosis in colon carcinoma cells.[48] Therefore, to further understand the secretome of hiNeuroS-TRAIL cells and how it impacts the tumors and their microenvironments, further investigation through DNA microarrays and RNA sequencing studies is required.

Notably, the combination treatment also significantly decreased the expression of IAPs (survivin and XIAP) and visibly decreased the anti-apoptotic protein, MCL-1 (Figure S2A) in LN229. Previous reports have suggested that the overexpression of survivin and XIAP are associated with radioresistance, chemoresistance, and TRAIL resistance in several cancers,[49–51] and that the inhibition of survivin and XIAP effectively sensitized GBM cells to apoptosis.[52] Moreover, the elevation of MCL-1 seems to be resistant to radiation, chemotherapy, and other treatments in several cancers.[53,54] Thus, the down-regulation of these biological markers suggests that the combination therapy could be incorporated with current standard-of-care treatments in patients with GBM, potentially increasing the sensitivity to radiation and chemotherapy. We demonstrated that combination therapy-induced changes within the apoptotic pathways, and our future studies will focus on RNA sequencing to elucidate the underlying mechanisms and the impact of each therapy individually or in combination to treat GBM.

To develop and translate the hiNeuroS-TRAIL/TR-107 combination therapy-induced effect *in vivo*, we first conducted dose optimization studies of single-agent therapies and further examined their combinatory treatment effects in a TRAIL-resistant LN229 GBM murine model and longitudinally tracked their tumor growths and monitored for survival outcome.[38] We found that mice treated with combination therapy demonstrated a significantly decreased the tumor growth rate compared with the control group and the survival outcome was

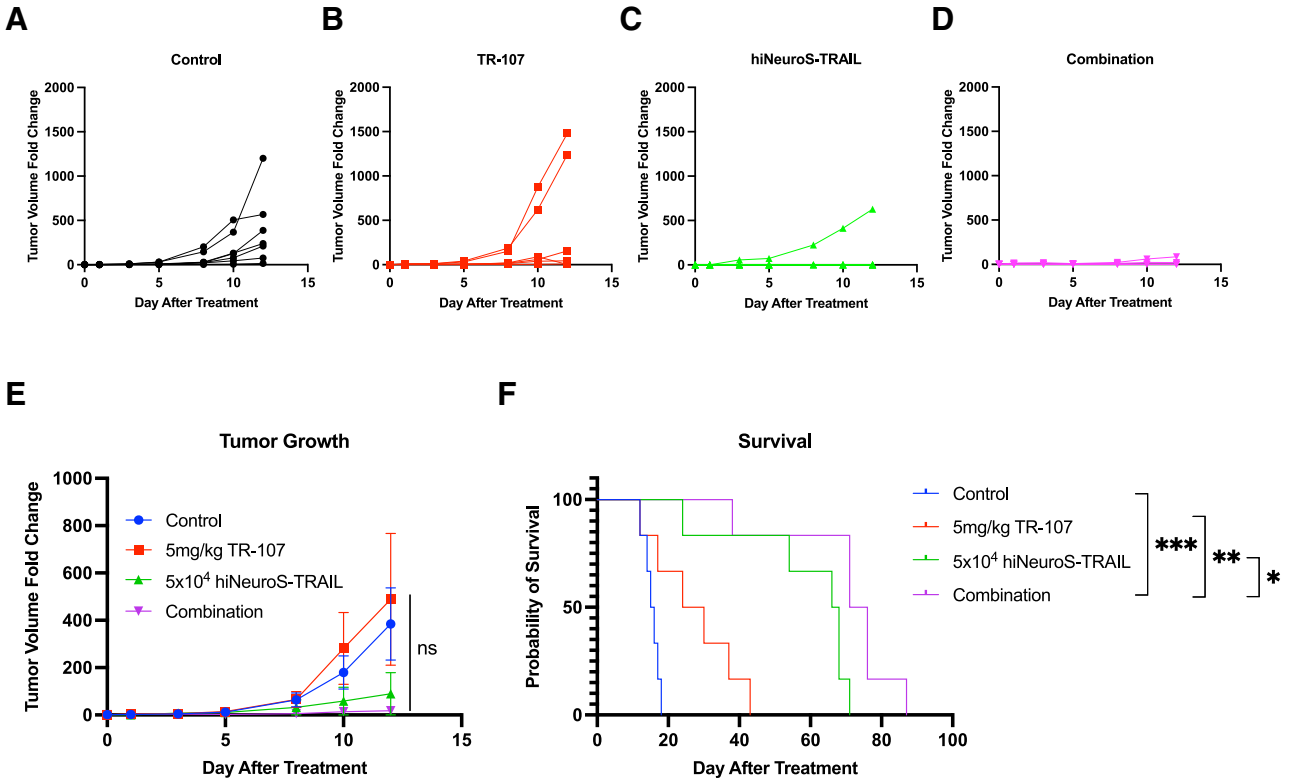

Figure 7. Combining TR-107 and hiNeuroS-TRAIL significantly improved survival outcome in an invasive murine model of GBM

(A–D) Individual mouse tumor growth data across all treatment groups from GBM8 *in vivo* efficacy experiment. (E) Fold change in tumor growth curves across all treatment groups. (F) Kaplan-Meier survival curve of mice treated with control, TR-107, hiNeuroS-TRAIL, or combination at indicated doses (n = 6–7). The data are represented as mean ± SEM (*$p < 0.05$, **$p < 0.01$, ***$p < 0.001$, ns = not significant).

significantly extended in the combination-treated mice compared with the control and single-agent treatment groups of mice.

To further assess the therapeutic efficacy of hiNeuroS-TRAIL/TR-107 combination therapy in an additional GBM mouse model to bolster our *in vivo* data, we selected a more invasive GBM8 model. Although it has been reported that GBM8 is extremely sensitive to TRAIL *in vitro* (also indicated in Figures 1F and 1I), GBM8 grows aggressively in mice.[39] Therefore, we decreased the cell counts of hiNeuroS-TRAIL in half while maintaining the same TR-107 dosing routine using this invasive model. Although no significant difference in the tumor growth rate was observed, survival of mice treated both single agents and combination treatments extended significantly compared with the control group. In addition, we found that combination therapy prolonged a significant survival outcome compared with all other treatment groups, indicating that continuous dosing of TR-107 was necessary to ultimately suppress hiNeuroS-TRAIL-mediated tumor recurrence. Together, these data suggest that the combination of TR-107 and hiNeuroS-TRAIL is a promising treatment regimen against GBM.

In this study, we used simple IT models to deliver and test our unique stem cell therapy in GBM mice. An advantage of our approach is that it avoided confounding factors such as cell migration and allowed us to solely assess the therapeutic effects of our combination therapy. However, to further evaluate potential clinical applications, our future studies will explore additional and clinically relevant methods for stem cell administration, such as infusing via an intracerebroventricular route, as well as implanting in surgically resected cavities by safely encapsulating hiNeuroS-TRAIL cells with a hemostatic matrix, FLOSEAL, which has been ap[proved by the U.S. Food and Drug Administration.[55]

Although several experiments are required to fully understand the anti-cancer mechanisms of these drugs, in this study we showed that combining hiNeuroS-TRAIL and TR-107 has significant clinical potential to treat high grade-gliomas by altering apoptotic pathways that are known to be involved in standard-of-care treatment and TRAIL resistance, potentially restoring radiation and chemotherapeutic sensitivity in GBM. Moreover, both therapies have the potential for rapid clinical translation because various TRAIL and TRAIL-related therapies have been evaluated in the clinical trials against several cancers.[7] In addition, ONC201, the parent compound for TR-107, is in phase 3 clinical trials for both adult and pediatric patients with the H3 K27M genetic mutation (NCT05580562).

TR-107 has been shown to be significantly more potent than ONC201 and is well tolerated in mice,[23] suggesting that it may be more efficacious than ONC201 in patients as well. Second, we have previously reported that our induced NSC therapy can be generated from patients' skin fibroblasts,[21] avoiding possible immune-related complications in the clinic. Hence, we believe that combining hiNeuroS-TRAIL and TR-107 is a promising combination therapy for clinical translation as these therapies can potentially mitigate the notorious limitations that hindered therapeutic outcomes in previous TRAIL-based clinical trials.

MATERIALS AND METHODS

Cell lines

LN229 cells were obtained through American Type Culture Collection. MS21 cells were derived from a GBM patient biopsy in the Hingtgen Laboratory. GBM8 cells were gifted by H. Wakimoto (Massachusetts General Hospital). LN229 and MS21 cells were cultured in 1× DMEM (Gibco) supplemented with 10% fetal bovine serum (FBS) and 1% penicillin-streptomycin (PenStrep) (10,000 units penicillin and 10 mg streptomycin/mL)—referred to as standard media. Both cell lines were incubated in 5% CO_2 at 37°C and passaged periodically using 0.05% Trypsin and centrifugation at 1,000×*g* for 5 min. GBM8 cells were cultured in EF media containing filtered 500 mL Neurobasal medium (Gibco) containing 3 mM L-glutamine, 10 mL B27 supplement, 2.5 mL N2 supplement, 2 μg/mL heparin, 1% PenStrep, 62.5 μg/mL amphotericin B, and 20 ng/mL of both epidermal growth factor and fibroblast growth factor in 5% CO_2 at 37°C. Before use, GBM8 cells were dissociated into single-cell suspension with Accutase.

hiNeuroS-TRAIL generation

hiNSCs were engineered to secrete TRAIL (hiNeuroS-TRAIL) as previously described (Wulin Jiang et al., 2021). hiNeuroS-TRAIL are cultured in ReNcell media and supplemented with doxycycline, epidermal growth factor, and fibroblast growth factor every other day. hiNeuroS-TRAIL cell line was incubated in 5% CO_2 at 37°C and passaged periodically using centrifugation. Before use, hiNeuroS-TRAIL cells were dissociated into a single-cell suspension with Accutase.

Lentiviral transduction

The following lentiviral vector encoding mCherry and firefly luciferase reporters (mCherry-Fluc) was prepared by Duke Viral Vector Core. The mCherry-Fluc lentiviral vector was used to transduce LN229, MS21, and GBM8 cell lines to longitudinally measure tumor fluorescence and bioluminescence signals *in vitro* and *in vivo* studies. Transduced GBM cell lines are indicated as LN229-mCh-Fluc, MS21-mCh-Fluc, and GBM8-mCh-Fluc.

TR-107 compound

TR-107 was generously provided by Dr. Edwin Iwanowicz and Madera Therapeutics, LLC, and was prepared as previously described (Emily Fennell et al., 2022). For IP injections, TR-107 was prepared first at 50 mM concentration in DMSO. From the 50-mM stocks, 1 mg/mL concentrations of TR-107 were prepared in solvent (5% Solutol in 1XPBS) for *in vivo* studies. For *in vitro* studies, appropriate dilutions were prepared in cell culture media.

In vitro efficacy studies

To perform *in vitro* efficacy assays, LN229 and MS21 cells were seeded in 96-well plates. We seeded 1.0×10^4 cells in 150 μL standard media each well and allowed to adhere to the plates for about 24 h (day 0). On day 1, the media was then aspirated, and various doses of TR-107 and amounts of hiNeuroS-TRAIL cells were added to each well in standard media. Cells in only standard media served as experimental controls. Doses of TR-107 were prepared by diluting 10 μM of TR-107 in standard media. Various hiNeuroS-TRAIL cell counts were prepared via centrifugation, dissociation with Accutase, and neutralization with 1× PBS. After resuspension in 1× PBS, 10 μL of cells were combined with 10 μL of Trypan blue and placed in counting chamber slides using Invitrogen Countess Cell Counter. Desired cell counts were calculated and resuspended in standard media for use. In treating GBM8 cells, the media was not aspirated 24 h after the cells were seeded as GBM8 cells grow in suspension. Thus, GBM8 cells were instead seeded in 100 μL EF media. After 24 h, the appropriate dose concentrations of TR-107 and cell counts of hiNeuroS-TRAIL were prepared in 50 μL EF media to bring up the total volumes to 150 μL. On day 4, termination assays were conducted using bioluminescent imaging (BLI) to quantify tumor signals by adding 150 μL 10% firefly-luciferin (prepared from 15 mg/mL stock solution) to each well of the treated 96-well plate. After 15 min of incubation, BLI images were captured using a Spectral Instruments AMI instrument with an exposure of 5 s. For synergy assays, the optimal doses (IC_{50}) for both therapies were combined on day 1, and their BLI signals were measured on day 4. CDI is calculated as CD = AB/(A*B) where AB is the ratio of combination two drugs compared with the control, A is the ratio of drug A compared with the control, and B is the ratio of drug B compared with the control. A synergistic effect is achieved when the CDI is <1, whereas a CDI of 1 indicates additive effect and a CDI of >1 indicates an antagonistic effect.[56]

Caspase Glo assays

Caspase Glo assay kits (Promega, Catalog #G8200, G8210, and G8090) were stored in −20°C and used following manufacturer directions. Briefly, the substrate and the buffer reagents were mixed thoroughly, and equal amounts of mixed reagent (100 μL) were added to experimental 96-well plates as instructed. The plates were then placed on a shaker for 30 s before incubating at 37°C for 1 hour. The BLI signals were recorded via AMI instrument and generated signals were then analyzed on Prism (GraphPad).

Western blot

We plated 1.0×10^5 LN229 cells in six-well plates with 3 mL of normal media per well for 24 h. The cells are then treated with 5.0×10^3 hiNeuroS-TRAIL, 100 nM TR-107, the combination of the two, and 100 nM of staurosporine as a positive control for 24 h. Following treatments, the media was aspirated, and the cells were rinsed three times with cold 1× PBS. The cells were then lysed in

RIPA buffer (20 mM Tris [pH 7.4], 127 mM NaCl, 10% glycerol, 1% Nonidet P-40, 0.5% deoxycholate, 2 mM EDTA) supplemented with 2 mM Na_3VO_4, 10 mM NaF, 0.0125 μM calyculin A, and cOmplete protease inhibitor cocktail (Roche Diagnostic, 11873580001).[23] Protein concentration of the cell lysates were quantified using the Bradford assay and diluted to 1 μg/μL in Laemmeli buffer and samples were loaded (20 μL/sample) and run on a 10% SDS-PAGE gel for 1 h at room temperature at 120 V. Samples were then transferred to a nitrocellulose membrane for 1 h at 4°C at 100 V. Membranes were incubated with a primary antibody (MCL-1 – Santa Cruz, Catalog #SC-819) diluted in 1% fish gelatin overnight at 4°C. The primary antibody was then removed, and the membranes were washed three times for 5 min in TBST before incubation in secondary antibody diluted in 5% milk for 1 h. The membranes were then washed three times for 10 min and were incubated in ECL reagent for 1 min. Images were acquired using a Chemidoc MP or Odyssey Fc.

Human apoptotic array

Proteome Profiler Human Apoptosis Array Kit (Catalog #: ARY009) was purchased from R&D Systems. 1.0×10^6 LN229 cells were seeded in 10-cm petri dishes for 24 h. The cells were then treated with regular media (1× DMEM with 10% FBS and 1% PenStrep), 1.0×10^5 hiNeuroS-TRAIL, 100 nM TR-107, and the combination of TR-107 and hiNeuroS-TRAIL. After 24 h, the cells were lysed using the lysis buffer provided with the kit, and the total proteins were further quantified. Nearly 200 μg cell lysates were used to further conduct the apoptotic array using the detailed protocol that was provided by R&D. The chemiluminescent blots were subsequently quantified using ImageJ software and analyzed on Prism (GraphPad) to determine the statistical differences.

In vivo solid tumor efficacy study

All animal studies conducted on female athymic nude mice were approved by the Institutional Animal Care and Use Committee at the University of North Carolina, Chapel Hill. Female athymic nude mice aged 6–8 weeks ($N = 7$) were intracranially implanted with 2.0×10^5 LN229-mCherry-FireflyLuciferase-expressing cells and the tumor growths were tracked via BLI (acquired on IVIS Kinetic, PerkinElmer) three times per week. During each acquisition, mice were injected with 15 mg/kg luciferin intraperitoneally. Mice from the four groups (control, TR-107, hiNeuroS-TRAIL, and combination) were randomized based on BLI signal to ensure that there was no statistical significance across groups before treatment. Seven days after tumor implantation, control mice received a single IT injection of 1XPBS on treatment day (day 0) and IP injections of vehicle (5% Solutol and 5% DMSO in 1× PBS) on experimental days 0, 2, 4, 14, 16, and 18. TR-107 mice received IP injections of 5 mg/kg TR-107 on experimental days 0, 2, 4, 14, 16, and 18. hiNeuroS-TRAIL group of mice received single IT injections of 1.0×10^5 hiNeuroS-TRAIL on day 0. For combination group, the mice were administered single IT injections of 1.0×10^5 hiNeuroS-TRAIL on day 0 and IP injections of 5 mg/kg TR-107 on experimental days 0, 2, 4, 14, 16, and 18. The tumor growths were tracked three times per week via BLI on the IVIS Spectrum and the signals were quantified in terms of tumor volume fold change from pre-treatment levels. Mice that met the parameters of humane endpoints were euthanized and were analyzed for survival outcome.

In vivo invasive tumor efficacy study

All animal studies conducted on female athymic nude mice were approved by the Institutional Animal Care and Use Committee at the University of North Carolina, Chapel Hill. Female athymic nude mice aged 6–8 weeks ($N = 6$) were intracranially implanted with 1.0×10^5 GBM-8-mCherry-FireflyLuciferase-expressing cells and the tumor burdens were tracked via bioluminescence imaging (acquired on IVIS Kinetic, PerkinElmer) three times per week. During each acquisition, mice were injected with 15 mg/kg luciferin intraperitoneally. Mice from the four groups (control, TR-107, hiNeuroS-TRAIL, and combination) were randomized based on BLI tumor signal to ensure that there was no statistical significance across treatment groups before treatment. Six days after tumor implantation, control mice received a single IT injection of 1× PBS on treatment day (day 0) and IP injections of vehicle (5% Solutol and 5% DMSO in 1× PBS) on experimental days 0, 2, 4, 14, 16, and 18 until the last mouse reached a humane endpoint. TR-107 mice received IP injections of 5 mg/kg TR-107 on experimental days 0, 2, 4, 14, 16, 18, 28, 30, 32, and 42 until the last mouse reached a humane endpoint. The hiNeuroS-TRAIL group of mice received single IT injections of 5.0×10^4 hiNeuroS-TRAIL on day 0. For the combination group, mice were administered single IT injections of 5.0×10^4 hiNeuroS-TRAIL on day 0 and IP injections of 5 mg/kg TR-107 on experimental days 0, 2, 4, 14, 16, 18, 28, 30, 32, 42, 44, 46, 56, 58, and 60. The tumor growths were tracked three times per week via BLI on IVIS Spectrum and the signals were quantified in tumor volume fold change. Mice that met the parameters of humane endpoints were euthanized and were analyzed for survival outcomes.

Graphics and statistical analysis

All schematics were generated using BioRender. All data were analyzed using GraphPad Prism software. Unpaired t tests were used when comparing two groups. One-way ANOVA was used to compare three or more groups with Tukey's multiple comparisons tests. Two-way ANOVA with mixed-effects analyses were used to compare two or more groups with different timepoints. Survival analyses were conducted using log rank (Mantel-Cox) tests. All values are expressed as ± SEM unless mentioned otherwise and the differences were considered significant when $p < 0.05$.

DATA AND CODE AVAILABILITY

All data for this publication are included in this paper as primary and the Supplemental figures. Additional data can be requested from the authors via email at morrent@unc.edu.

SUPPLEMENTAL INFORMATION

Supplemental information can be found online at https://doi.org/10.1016/j.omton.2024.200834.

ACKNOWLEDGMENTS

This work was supported by a T32 funding award through the neuroscience program at University of North Carolina at Chapel Hill, the Eshelman Institute for Innovation at University of North Carolina at Chapel Hill, and the National Cancer Institute of the National Institutes of Health under Award Number F30CA243270. We gratefully acknowledge Dr. Edwin Iwanowicz and Madera Therapeutics for providing the TR-107 compound. The content does not represent the official views of the National Institutes of Health.

AUTHOR CONTRIBUTIONS

M.T. led with project conceptualization, data curation, investigation, methodology, writing, reviewing, and editing. C.M. supported with data curation, investigation, methodology, writing, and reviewing. L.E.K. supported with data curation, methodology, reviewing, and editing. S.D. supported with data curation, methodology, writing, reviewing, and editing. E.M.J.F. supported with data curation, methodology, writing, reviewing, and editing. B.E.M. supported with data curation, reviewing, and editing. A.R.M.-S. supported with writing, reviewing, and editing. A.V. supported with data curation, reviewing, and editing. L.M.G. contributed with project conceptualization, resources, methodology, reviewing, and editing. S.D.H. contributed with project conceptualization, methodology, writing, reviewing, and editing.

DECLARATION OF INTERESTS

S.D.H. has ownership interest as the CSO of Falcon Therapeutics.

REFERENCES

1. Oronsky, B., Reid, T.R., Oronsky, A., Sandhu, N., and Knox, S.J. (2020). A Review of Newly Diagnosed Glioblastoma. Front. Oncol. *10*, 574012. https://doi.org/10.3389/fonc.2020.574012.
2. Hanif, F., Muzaffar, K., Perveen, K., Malhi, S.M., and Simjee, S.U. (2017). Glioblastoma Multiforme: A Review of its Epidemiology and Pathogenesis through Clinical Presentation and Treatment. Asian Pac. J. Cancer Prev. APJCP *18*, 3–9.
3. Baid, U., Rane, S.U., Talbar, S., Gupta, S., Thakur, M.H., Moiyadi, A., and Mahajan, A. (2020). Overall Survival Prediction in Glioblastoma with Radiomic Features Using Machine Learning. Front. Comput. Neurosci. *14*, 61.
4. Fernandez, C., Costa, A., Osorio, L., Costa Lago, R., Linhares, P., Carvalho, B., and Caeiro, C. (2017). Glioblastoma - Current Standards of Care in Glioblastoma Therapy (Ch11) (Codon Publications).
5. Tan, A.C., Ashley, D.M., López, G.Y., Malinzak, M., Friedman, H.S., and Khasraw, M. (2020). Management of glioblastoma: State of the art and future directions. CA A Cancer J. Clin. *70*, 299–312.
6. Snajdauf, M., Havlova, K., Vachtenheim, J., Ozaniak, A., Lischke, R., Bartunkova, J., Smrz, D., and Strizova, Z. (2021). The TRAIL in the Treatment of Human Cancer: An Update on Clinical Trials. Front. Mol. Biosci. *8*, 628332.
7. Thang, M., Mellows, C., Mercer-Smith, A., Nguyen, P., and Hingtgen, S. (2023). Current approaches in enhancing TRAIL therapies in glioblastoma. Neurooncol. Adv. *5*, vdad047.
8. Razeghian, E., Suksatan, W., Rahman, H.S., Bokov, D.O., Abdelbasset, W.K., Hassanzadeh, A., Marofi, F., Yazdanifar, M., and Jarahian, M. (2021). Harnessing TRAIL-Induced Apoptosis Pathway for Cancer Immunotherapy and Associated Challenges. Front. Immunol. *12*, 1–22.
9. Almasan, A., and Ashkenazi, A. (2003). Apo2L/TRAIL: Apoptosis signaling, biology, and potential for cancer therapy. Cytokine Growth Factor Rev. *14*, 337–348.
10. Oikonomou, E., and Pintzas, A. (2013). The TRAIL of oncogenes to apoptosis. Biofactors *39*, 343–354.
11. Lincz, L.F., Yeh, T.-X., and Spencer, A. (2001). TRAIL-induced eradication of primary tumour cells from multiple myeloma patient bone marrows is not related to TRAIL receptor expression or prior chemotherapy. Leukemia *15*, 1650–1657. www.nature.com/leu.
12. Zhang, Y., Dube, C., Gibert, M., Cruickshanks, N., Wang, B., Coughlan, M., Deveau, C., Saoud, K., Yang, Y., Setiady, I., et al. (2018). The p53 pathway in glioblastoma. Cancers *10*, 297. https://doi.org/10.3390/cancers10090297.
13. Breen, L., Heenan, M., Amberger-Murphy, V., and Clynes, M. (2007). Investigation of the Role of p53 in Chemotherapy Resistance of Lung Cancer Cell Lines. Anticancer Res. *27*, 1361–1364.
14. Thapa, B., KC, R., and Uludağ, H. (2020). TRAIL Therapy and Prospective Developments for Cancer Treatment. J. Contr. Release *326*, 335–349.
15. De Miguel, D., Lemke, J., Anel, A., Walczak, H., and Martinez-Lostao, L. (2016). Onto better TRAILs for cancer treatment. Cell Death Differ. *23*, 733–747.
16. Holland, P.M. (2014). Death receptor agonist therapies for cancer, which is the right TRAIL? Cytokine Growth Factor Rev. *25*, 185–193.
17. Bagó, J.R., Okolie, O., Dumitru, R., Ewend, M.G., Parker, J.S., Vander Werff, R., Underhill, T.M., Schmid, R.S., Miller, C.R., and Hingtgen, S.D. (2017). Tumor-homing Cytotoxic Human Induced Neural Stem Cells for Cancer Therapy, *9*, pp. 1–25.
18. Mercer-Smith, A.R., Buckley, A., Valdivia, A., Jiang, W., Thang, M., Bell, B., Kumar, R.J., Bomba, H.N., Woodell, A.S., Luo, J., et al. (2022). Next-generation Tumor-homing Induced Neural Stem Cells as an Adjuvant to Radiation for the Treatment of Metastatic Lung Cancer. Stem Cell Rev. Rep. *18*, 2474–2493.
19. Jiang, W., Yang, Y., Mercer-Smith, A.R., Valdivia, A., Bago, J.R., Woodell, A.S., Buckley, A.A., Marand, M.H., Qian, L., Anders, C.K., and Hingtgen, S.D. (2021). Development of next-generation tumor-homing induced neural stem cells to enhance treatment of metastatic cancers. Sci. Adv. *7*, eabf1526.
20. Morizane, A., Doi, D., Kikuchi, T., Okita, K., Hotta, A., Kawasaki, T., Hayashi, T., Onoe, H., Shiina, T., Yamanaka, S., and Takahashi, J. (2013). Direct comparison of autologous and allogeneic transplantation of IPSC-derived neural cells in the brain of a nonhuman primate. Stem Cell Rep. *1*, 283–292.
21. Buckley, A., Hagler, S.B., Lettry, V., Bagó, J.R., Maingi, S.M., Khagi, S., Ewend, M.G., Miller, C.R., and Hingtgen, S.D. (2020). Generation and Profiling of Tumor-Homing Induced Neural Stem Cells from the Skin of Cancer Patients. Mol. Ther. *28*, 1614–1627.
22. Deng, L., Zhai, X., Liang, P., and Cui, H. (2021). Overcoming trail resistance for glioblastoma treatment. Biomolecules *11*, 572–617.
23. Fennell, E.M.J., Aponte-Collazo, L.J., Wynn, J.D., Drizyte-Miller, K., Leung, E., Greer, Y.E., Graves, P.R., Iwanowicz, A.A., Ashamalla, H., Holmuhamedov, E., et al. (2022). Characterization of TR-107, a novel chemical activator of the human mitochondrial protease ClpP. Pharmacol. Res. Perspect. *10*, e00993.
24. Arrillaga-Romany, I., Lassman, A., Mcgovern, S., Mueller, S., Nabors, L.B., Van Den Bent, M., Vogelbaum, M., Allen, J.E., Melemed, A., Tarapore, R., et al. (2022). A Randomized Phase 3 Study of ONC201 in Patients with Newly Diagnosed H3 K27M-Mutant Diffuse Glioma. https://academic.oup.com/neuro-oncology/article/24/Supplement_7/vii249/6826555.
25. Jackson, E.R., Duchatel, R.J., Staudt, D.E., Persson, M.L., Mannan, A., Yadavilli, S., Parackal, S., Game, S., Chong, W.C., Jayasekara, W.S.N., et al. (2023). ONC201 in Combination with Paxalisib for the Treatment of H3K27-Altered Diffuse Midline Glioma. Cancer Res. OF1–OF17.
26. Free, R.B., Cuoco, C.A., Xie, B., Namkung, Y., Prabhu, V.V., Willette, B.K.A., Day, M.M., Sanzhez-Soto, M., Lane, J.R., A Laporte, S., et al. (2021). Pharmacological Characterization of the Imipridone Anti-Cancer Drug ONC201 Reveals a Negative Allosteric Mechanism of Action at the D2 Dopamine Receptor. Mol. Pharmacol. *100*, 372–387.
27. Ralff, M.D., Lulla, A.R., Wagner, J., and El-Deiry, W.S. (2017). ONC201: A New Treatment Option Being Tested Clinically for Recurrent Glioblastoma. Transl. Cancer Res. *6*, S1239–S1243.
28. Graves, P.R., Aponte-Collazo, L.J., Fennell, E.M.J., Graves, A.C., Hale, A.E., Dicheva, N., Herring, L.E., Gilbert, T.S.K., East, M.P., McDonald, I.M., et al. (2019).

Mitochondrial Protease ClpP is a Target for the Anticancer Compounds ONC201 and Related Analogues. ACS Chem. Biol. *14*, 1020–1029.

29. Ishizawa, J., Zarabi, S.F., Davis, R.E., Halgas, O., Nii, T., Jitkova, Y., Zhao, R., St-Germain, J., Heese, L.E., Egan, G., et al. (2019). Mitochondrial ClpP-Mediated Proteolysis Induces Selective Cancer Cell Lethality. Cancer Cell *35*, 721–737.e9.
30. Mabanglo, M.F., Wong, K.S., Barghash, M.M., Leung, E., Chuang, S.H.W., Ardalan, A., Majaesic, E.M., Wong, C.J., Zhang, S., Lang, H., et al. (2023). Potent ClpP Agonists with Anticancer Properties Bind with Improved Structural Complementarity and Alter the Mitochondrial N-terminome. Structure *31*, 185–200.e10.
31. Greer, Y.E., Porat-Shliom, N., Nagashima, K., Stuelten, C., Crooks, D., Koparde, V.N., Gilbert, S.F., Islam, C., Ubaldini, A., Ji, Y., et al. (2018). ONC201 kills breast cancer cells *in vitro* by targeting mitochondria. Oncotarget *9*, 18454–18479. www.oncotarget.com.
32. Wedam, R., Greer, Y.E., Wisniewski, D.J., Weltz, S., Kundu, M., Voeller, D., and Lipkowitz, S. (2023). Targeting Mitochondria with ClpP Agonists as a Novel Therapeutic Opportunity in Breast Cancer. Cancers *15*, 1936. https://doi.org/10.3390/cancers15071936.
33. Jhaveri, A.V., Zhou, L., Ralff, M.D., Lee, Y.S., Navaraj, A., Carneiro, B.A., Safran, H., Prabhu, V.V., Ross, E.A., Lee, S., et al. (2021). Combination of ONC201 and TLY012 induces selective, synergistic apoptosis *in vitro* and significantly delays PDAC xenograft growth *in vivo*. Cancer Biol. Ther. *22*, 607–618.
34. He, L., Bhat, K., Ioannidis, A., Zhang, L., Nguyen, N.T., Allen, J.E., Nghiemphu, P.L., Cloughesy, T.F., Liau, L.M., Kornblum, H.I., and Pajonk, F. (2021). Effects of the DRD2/3 antagonist ONC201 and radiation in glioblastoma. Radiother. Oncol. *161*, 140–147.
35. Stella, N., Diaz, P., Horne, E., Xu, C., Hamel, E., Wagenbach, M., Petrov, R., Hass, B., Parvinder, H., Wordeman, L., et al. (2018). Modified Carbazoles Destabilize Microtubules and Kill Glioblastoma Multiform Cells.
36. Lim, B., Peterson, C.B., Davis, A., Cho, E., Pearson, T., Liu, H., Hwang, M., Ueno, N.T., and Lee, J. (2021). ONC201 and an MEK Inhibitor Trametinib Synergistically Inhibit the Growth of Triple-Negative Breast Cancer Cells. Biomedicines *9*, 1410.
37. Zhao, Z., Mei, Y., Wang, Z., and He, W. (2022). The Effect of Oxidative Phosphorylation on Cancer Drug Resistance. Cancers *15*, 62. https://doi.org/10.3390/cancers15010062.
38. Redjal, N., Zhu, Y., and Shah, K. (2015). Combination of systemic chemotherapy with local stem cell delivered S-TRAIL in resected brain tumors. Stem Cell. *33*, 101–110.
39. Satterlee, A.B., Dunn, D.E., Valdivia, A., Malawsky, D., Buckley, A., Gershon, T., Floyd, S., and Hingtgen, S. (2022). Spatiotemporal analysis of induced neural stem cell therapy to overcome advanced glioblastoma recurrence. Mol. Ther. Oncolytics *26*, 49–62.
40. Wang, S., and El-Deiry, W.S. (2003). TRAIL and apoptosis induction by TNF-family death receptors. Oncogene *22*, 8628–8633. https://doi.org/10.1038/sj.onc.1207232.
41. Cavalcante, G.C., Schaan, A.P., Cabral, G.F., Santana-Da-Silva, M.N., Pinto, P., Vidal, A.F., and Ribeiro-Dos-Santos, Â. (2019). A cell's fate: An overview of the molecular biology and genetics of apoptosis. Int. J. Mol. Sci. *20*, 4133. https://doi.org/10.3390/ijms20174133.
42. Cheung, C.H.A., Chang, Y.C., Lin, T.Y., Cheng, S.M., and Leung, E. (2020). Anti-apoptotic proteins in the autophagic world: An update on functions of XIAP, Survivin, and BRUCE. J. Biomed. Sci. *27*, 31. https://doi.org/10.1186/s12929-020-0627-5.
43. Ghosh, D., Nandi, S., and Bhattacharjee, S. (2018). Combination therapy to checkmate Glioblastoma: clinical challenges and advances. Clin. Transl. Med. *7*, 33.
44. Zhao, M., van Straten, D., Broekman, M.L.D., Préat, V., and Schiffelers, R.M. (2020). Nanocarrier-based drug combination therapy for glioblastoma. Theranostics *10*, 1355–1372. https://doi.org/10.7150/thno.38147.
45. Ralff, M.D., and El-Deiry, W.S. (2018). TRAIL pathway targeting therapeutics. Expert Rev. Precis. Med. Drug Dev. *3*, 197–204. https://doi.org/10.1080/23808993.2018.1476062.
46. Wiley, S.R., Schooley, K., Smolak, P.J., Din, W.S., Huang, C.P., Nicholl, J.K., Sutherland, G.R., Smith, T.D., Rauch, C., Smith, C.A., et al. (1995). Identification and characterization of a new member of the TNF family that induces apoptosis. Immunity *3*, 673–682.
47. Khodayar, M.J., Rezaei Tazangi, F., Samimi, A., and Alidadi, H. (2023). Adipose-Derived Mesenchymal Stem Cells Secretome Induces Apoptosis in Colon Carcinoma HT-29 Cells. Jentashapir J. Cell. Mol. Biol. *13*.
48. Vaseva, A.V., and Moll, U.M. (2009). The Mitochondrial p53 Pathway. Biochim. Biophys. Acta *1787*, 414–420. https://doi.org/10.1016/j.bbabio.2008.10.005.
49. Dong, X., Liu, W., Li, X., Gan, Y., Zhou, L., Li, W., and Xie, L. (2022). Butein promotes ubiquitination-mediated survivin degradation inhibits tumor growth and overcomes chemoresistance. Sci. Rep. *12*, 20644.
50. Devi, G.R., Finetti, P., Morse, M.A., Lee, S., de Nonneville, A., Van Laere, S., Troy, J., Geradts, J., McCall, S., and Bertucci, F. (2021). Expression of x-linked inhibitor of apoptosis protein (Xiap) in breast cancer is associated with shorter survival and resistance to chemotherapy. Cancers *13*, 2807.
51. Chawla-Sarkar, M., Bae, S.I., Reu, F.J., Jacobs, B.S., Lindner, D.J., and Borden, E.C. (2004). Downregulation of Bcl-2, FLIP or IAPs (XIAP and survivin) by siRNAs sensitizes resistant melanoma cells to Apo2L/TRAIL-induced apoptosis. Cell Death Differ. *11*, 915–923.
52. Valdés-Rives, S.A., Casique-Aguirre, D., Germán-Castelán, L., Velasco-Velázquez, M.A., and González-Arenas, A. (2017). Apoptotic Signaling Pathways in Glioblastoma and Therapeutic Implications. BioMed Res. Int. *2017*, 7403747. https://doi.org/10.1155/2017/7403747.
53. Bolomsky, A., Vogler, M., Köse, M.C., Heckman, C.A., Ehx, G., Ludwig, H., and Caers, J. (2020). MCL-1 inhibitors, fast-lane development of a new class of anti-cancer agents. J. Hematol. Oncol. *13*, 173. https://doi.org/10.1186/s13045-020-01007-9.
54. Wu, X., Luo, Q., and Liu, Z. (2020). Ubiquitination and deubiquitination of MCL1 in cancer: deciphering chemoresistance mechanisms and providing potential therapeutic options. Cell Death Dis. *11*, 556. https://doi.org/10.1038/s41419-020-02760-y.
55. Bomba, H.N., Carey-Ewend, A., Sheets, K.T., Valdivia, A., Goetz, M., Findlay, I.A., Mercer-Smith, A., Kass, L.E., Khagi, S., and Hingtgen, S.D. (2022). Use of FLOSEAL® as a scaffold and its impact on induced neural stem cell phenotype, persistence, and efficacy. Bioeng. Transl. Med. *7*, e10283.
56. Chen, L., Ye, H., Zhang, G., Yao, W., Chen, X., Zhang, F., and Liang, G. (2014). Autophagy inhibition contributes to the synergistic interaction between EGCG and doxorubicin to kill the hepatoma Hep3B cells. PLoS One *9*, e85771.